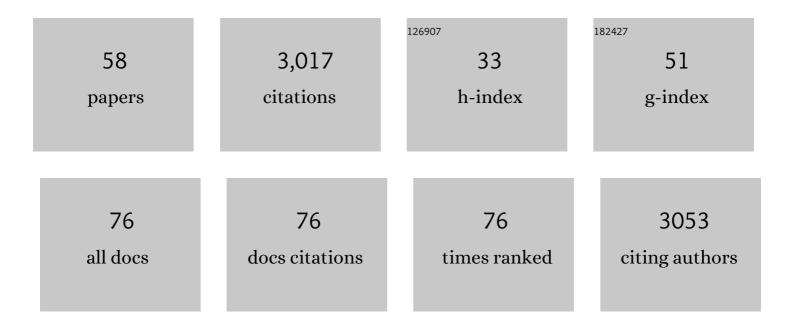
List of Publications by Year in descending order

Source: https://exaly.com/author-pdf/3690493/publications.pdf

Version: 2024-02-01



#	Article	IF	CITATIONS
1	Subpixel heterogeneity of ice-wedge polygonal tundra: a multi-scale analysis of land cover and evapotranspiration in the Lena River Delta, Siberia. Tellus, Series B: Chemical and Physical Meteorology, 2022, 64, 17301.	1.6	94
2	Novel coupled permafrost–forest model (LAVESI–CryoGrid v1.0) revealing the interplay between permafrost, vegetation, and climate across eastern Siberia. Geoscientific Model Development, 2022, 15, 2395-2422.	3.6	7
3	Thermohydrological Impact of Forest Disturbances on Ecosystemâ€Protected Permafrost. Journal of Geophysical Research G: Biogeosciences, 2022, 127, .	3.0	3
4	Variability of the surface energy balance in permafrost-underlain boreal forest. Biogeosciences, 2021, 18, 343-365.	3.3	19
5	Climate change reduces winter overland travel across the Pan-Arctic even under low-end global warming scenarios. Environmental Research Letters, 2021, 16, 024049.	5.2	20
6	Effects of multi-scale heterogeneity on the simulated evolution of ice-rich permafrost lowlands under a warming climate. Cryosphere, 2021, 15, 1399-1422.	3.9	16
7	Simulating Snow Redistribution and its Effect on Ground Surface Temperature at a Highâ€Arctic Site on Svalbard. Journal of Geophysical Research F: Earth Surface, 2021, 126, e2020JF005673.	2.8	20
8	Consequences of permafrost degradation for Arctic infrastructure – bridging the model gap between regional and engineering scales. Cryosphere, 2021, 15, 2451-2471.	3.9	42
9	Surface temperatures and their influence on the permafrost thermal regime in high-Arctic rock walls on Svalbard. Cryosphere, 2021, 15, 2491-2509.	3.9	7
10	Monitoring the Transformation of Arctic Landscapes: Automated Shoreline Change Detection of Lakes Using Very High Resolution Imagery. Remote Sensing, 2021, 13, 2802.	4.0	5
11	Lateral thermokarst patterns in permafrost peat plateaus in northern Norway. Cryosphere, 2021, 15, 3423-3442.	3.9	11
12	A Quantitative Graph-Based Approach to Monitoring Ice-Wedge Trough Dynamics in Polygonal Permafrost Landscapes. Remote Sensing, 2021, 13, 3098.	4.0	12
13	Sensitivity of ecosystem-protected permafrost under changing boreal forest structures. Environmental Research Letters, 2021, 16, 084045.	5.2	11
14	Fast response of cold ice-rich permafrost in northeast Siberia to a warming climate. Nature Communications, 2020, 11, 2201.	12.8	134
15	Multitemporal terrestrial laser scanning point clouds for thaw subsidence observation at Arctic permafrost monitoring sites. Earth Surface Processes and Landforms, 2020, 45, 1589-1600.	2.5	17
16	Pathways of ice-wedge degradation in polygonal tundra under different hydrological conditions. Cryosphere, 2019, 13, 1089-1123.	3.9	46
17	Thaw processes in ice-rich permafrost landscapes represented with laterally coupled tiles in a land surface model. Cryosphere, 2019, 13, 591-609.	3.9	57
18	Size Distributions of Arctic Waterbodies Reveal Consistent Relations in Their Statistical Moments in Space and Time. Frontiers in Earth Science. 2019. 7	1.8	25

#	Article	IF	CITATIONS
19	Improving Permafrost Modeling by Assimilating Remotely Sensed Soil Moisture. Water Resources Research, 2019, 55, 1814-1832.	4.2	22
20	A long-term (2002 to 2017) record of closed-path and open-path eddy covariance CO ₂ net ecosystem exchange fluxes from the Siberian Arctic. Earth System Science Data, 2019, 11, 221-240.	9.9	20
21	A 16-year record (2002–2017) of permafrost, active-layer, and meteorological conditions at the Samoylov Island Arctic permafrost research site, Lena River delta, northern Siberia: an opportunity to validate remote-sensing data and land surface, snow, and permafrost models. Earth System Science Data. 2019. 11. 261-299.	9.9	69
22	Borehole temperature reconstructions reveal differences in past surface temperature trends for the permafrost in the Laptev Sea region, Russian Arctic. Arktos, 2018, 4, 1-17.	1.0	5
23	Observation and modelling of snow at a polygonal tundra permafrost site: spatial variability and thermal implications. Cryosphere, 2018, 12, 3693-3717.	3.9	33
24	Thaw Subsidence of a Yedoma Landscape in Northern Siberia, Measured In Situ and Estimated from TerraSAR-X Interferometry. Remote Sensing, 2018, 10, 494.	4.0	69
25	Lakeâ€Atmosphere Heat Flux Dynamics of a Thermokarst Lake in Arctic Siberia. Journal of Geophysical Research D: Atmospheres, 2018, 123, 5222-5239.	3.3	10
26	Permafrost Thaw and Liberation of Inorganic Nitrogen in Eastern Siberia. Permafrost and Periglacial Processes, 2017, 28, 605-618.	3.4	43
27	Transient modeling of the ground thermal conditions using satellite data in the Lena River delta, Siberia. Cryosphere, 2017, 11, 1441-1463.	3.9	41
28	Carbon stocks and fluxes in the high latitudes: using site-level data to evaluate Earth system models. Biogeosciences, 2017, 14, 5143-5169.	3.3	43
29	PeRL: aÂcircum-Arctic Permafrost Region Pond andÂLakeÂdatabase. Earth System Science Data, 2017, 9, 317-348.	9.9	62
30	Monitoring Bedfast Ice and Ice Phenology in Lakes of the Lena River Delta Using TerraSAR-X Backscatter and Coherence Time Series. Remote Sensing, 2016, 8, 903.	4.0	32
31	Simulating the thermal regime and thaw processes of ice-rich permafrost ground with the land-surface model CryoGrid 3. Geoscientific Model Development, 2016, 9, 523-546.	3.6	104
32	Rapid degradation of permafrost underneath waterbodies in tundra landscapes—Toward a representation of thermokarst in land surface models. Journal of Geophysical Research F: Earth Surface, 2016, 121, 2446-2470.	2.8	54
33	SMOS prototype algorithm for detecting autumn soil freezing. Remote Sensing of Environment, 2016, 180, 346-360.	11.0	109
34	Spatio-temporal variability of X-band radar backscatter and coherence over the Lena River Delta, Siberia. Remote Sensing of Environment, 2016, 182, 169-191.	11.0	30
35	Satellite-derived changes in the permafrost landscape of central Yakutia, 2000–2011: Wetting, drying, and fires. Global and Planetary Change, 2016, 139, 116-127.	3.5	69
36	Impact of model developments on present and future simulations of permafrost in a global land-surface model. Cryosphere, 2015, 9, 1505-1521.	3.9	54

#	Article	IF	CITATIONS
37	Thermal processes of thermokarst lakes in the continuous permafrost zone of northern Siberia – observations and modeling (Lena River Delta, Siberia). Biogeosciences, 2015, 12, 5941-5965.	3.3	38
38	Site-level model intercomparison of high latitude and high altitude soil thermal dynamics in tundra and barren landscapes. Cryosphere, 2015, 9, 1343-1361.	3.9	41
39	An improved representation of physical permafrost dynamics in the JULES land-surface model. Geoscientific Model Development, 2015, 8, 1493-1508.	3.6	79
40	Spatio-temporal sensitivity of MODIS land surface temperature anomalies indicates high potential for large-scale land cover change detection in Arctic permafrost landscapes. Remote Sensing of Environment, 2015, 168, 1-12.	11.0	58
41	Frozen ponds: production and storage of methane during the Arctic winter in a lowland tundra landscape in northern Siberia, Lena River delta. Biogeosciences, 2015, 12, 977-990.	3.3	58
42	Simulating high-latitude permafrost regions by the JSBACH terrestrial ecosystem model. Geoscientific Model Development, 2014, 7, 631-647.	3.6	109
43	Freeze/thaw processes in complex permafrost landscapes of northern Siberia simulated using the TEM ecosystem model: impact of thermokarst ponds and lakes. Geoscientific Model Development, 2014, 7, 1671-1689.	3.6	39
44	Low Cost, Mobile Sensor System for Measurement of Carbon Dioxide in Permafrost Areas. Procedia Engineering, 2014, 87, 1318-1321.	1.2	3
45	Latent heat exchange in the boreal and arctic biomes. Global Change Biology, 2014, 20, 3439-3456.	9.5	52
46	Satellite-based modeling of permafrost temperatures in a tundra lowland landscape. Remote Sensing of Environment, 2013, 135, 12-24.	11.0	91
47	Spatial and seasonal variability of polygonal tundra water balance: Lena River Delta, northern Siberia (Russia). Hydrogeology Journal, 2013, 21, 133-147.	2.1	71
48	Baseline characteristics of climate, permafrost and land cover from a new permafrost observatory in the Lena River Delta, Siberia (1998–2011). Biogeosciences, 2013, 10, 2105-2128.	3.3	144
49	Systematic bias of average winter-time land surface temperatures inferred from MODIS at a site on Svalbard, Norway. Remote Sensing of Environment, 2012, 118, 162-167.	11.0	75
50	Permafrost $\hat{a} \in $ Physical Aspects, Carbon Cycling, Databases and Uncertainties. , 2012, , 159-185.		20
51	Small ponds with major impact: The relevance of ponds and lakes in permafrost landscapes to carbon dioxide emissions. Global Biogeochemical Cycles, 2012, 26, .	4.9	131
52	Spatial and temporal variations of summer surface temperatures of high-arctic tundra on Svalbard — Implications for MODIS LST based permafrost monitoring. Remote Sensing of Environment, 2011, 115, 908-922.	11.0	97
53	The surface energy balance of a polygonal tundra site in northern Siberia – Part 2: Winter. Cryosphere, 2011, 5, 509-524.	3.9	63
54	The surface energy balance of a polygonal tundra site in northern Siberia – Part 1: Spring to fall. Cryosphere, 2011, 5, 151-171.	3.9	77

#	Article	IF	CITATIONS
55	Modeling the impact of wintertime rain events on the thermal regime of permafrost. Cryosphere, 2011, 5, 945-959.	3.9	95
56	Spatial and temporal variations of summer surface temperatures of wet polygonal tundra in Siberia - implications for MODIS LST based permafrost monitoring. Remote Sensing of Environment, 2010, 114, 2059-2069.	11.0	74
57	The annual surface energy budget of a high-arctic permafrost site on Svalbard, Norway. Cryosphere, 2009, 3, 245-263.	3.9	104
58	Serpentine (Floating) Ice Channels and their Interaction with Riverbed Permafrost in the Lena River Delta, Russia. Frontiers in Earth Science, 0, 9, .	1.8	10